Article

Cyclodextrin Derivatives Conjugated with Aromatic Moieties as pH-Responsive Drug Carriers for Anthracycline.

Olga Swiech, Paula Dutkiewicz, Karolina Ewa Wójciuk, Kazimierz Z Chmurski, Marcin Kruszewski, and Renata Bilewicz

J. Phys. Chem. B, **Just Accepted Manuscript** • Publication Date (Web): 30 Sep 2013

Cyclodextrin Derivatives Conjugated with Aromatic Moieties as pH-responsive Drug Carriers for Anthracycline.

Olga Swiech[a], Paula Dutkiewicz[a], Karolina Wójciuk[b], Kazimierz Chmurski[a], Marcin Kruszewski[b,c], Renata Bilewicz[a].*

[a] University of Warsaw, Faculty of Chemistry, Pasteura 1, Warsaw, Poland

[b] Institute of Nuclear Chemistry and Technology, Dorodna 16, Warsaw, Poland

[c] Institute of Rural Health, Jaczewskiego 2, Lublin, Poland.

Abstract

The modification of cyclodextrins (CDs) with a side chain containing aromatic group lead to an increase of the stability of the complex with the anticancer drug - doxorubicin (Dox). The formation constant evaluated by voltammetry was several orders of magnitude larger compared to that of the unmodified βCD ligand. For the CDs with aromatic moieties connected by linkers containing triazole group, the formation constants of the complexes at pH 5.5 and 7.4 were very different. At lower pH, binding was much weaker due to protonation of the triazole moiety in the linker. The drug was then released from the complex. Molecular modeling of the Dox–βCD system revealed different interactions possible between Dox and βCD. The observed pH dependence of the complex formation constant can be exploited for drug delivery to the targeted cells. Toxicity of the synthesized complex and each

of the complex components were tested by the MTT assay on two cell lines, the human lung carcinoma and the human cervical cancer cell lines.

Keywords: cyclodextrin, doxorubicin, drug delivery system, anthracycline, drug complexation, drug toxicity.

Introduction

Anthracycline drugs have been used for nearly forty years for a treatment of several malignancies and hundreds of analogs of the first anthracycline antibiotics: doxorubicin (Dox) and daunorubicin have been synthesized and evaluated. Clinical treatment with anthracycline chemotherapeutics is limited by severe adverse effects such as cardiotoxicity and myelosupression [1,2,3]. In this context, tumor drug targeting has proven as a new, promising strategy to increase local drug concentration and to reduce unwanted side effects.

The specific toxicity of the anthracycline drugs is due to the reactive forms of oxygen: superoxide anion radical, hydrogen peroxide, and very reactive hydroxyl radical, which are produced in redox reactions of anthracyclines, such as Fenton reaction, where antracyclines create complex with free iron cations by anthraquinone group [4, 5, 6] . This specific toxicity can be reduced by creating a complex between anthracycline molecule and cyclodextrin (CD). In addition, Dox is not stable in aqueous solution due to its photosensitivity [7,8]. However, the Dox stability can be enhanced by complexing with CDs. Formation of the complex between Dox and both β- and γ-CDs has been proved by variety of methods, including fluorescence, absorbance, circular dichroism, and NMR [9]. In the complex, the anthraquinone group of the drug is located inside the CD cavity, resulting in a significantly slower rate of degradation [10]. The limitation in the use of CD as a carrier of anthracycline drugs is the low stability constant of the complex compared with that of the drug-DNA

complex [11]. Conjugation of CDs with appropriate moieties is proposed as a strategy towards complex controlled target drug carriers [12,13,14].

Recently, we have shown that the modification of CD with appropriate aromatic groups can significantly increase their drug-inclusion ability. The stability constants of the Dox complexes with the CD derivatives that have a single pendant 4-methoxyphenyl-terminated arm are 2−3 orders of magnitude larger than those of the complexes with native βCD. Moreover, the complex formation depends on the solvent. The formation of the inclusion complex takes place in the presence of water, while in aprotic solvents the complex is not formed because Dox cannot compete with the side chain of CD for the place in the cavity [15].

Studies of the tumor cells show that the pH of interstitial fluid surrounding the tumor is lower than the pH of normal cells [16,17]. This difference of pH has been exploiting in designing new pH-dependent drug carriers. Li and coworkers investigated a pH-responsive binding behavior of β-carboline derivative of βCD containing ethanediamine linker with Dox [18]. Using MS, NMR and fluorescence spectra authors proved that change of pH from 7.4 to 5.5 results in the release of drug from the cavity of the CD. The modification of CDs by β-carboline group increases the stability constants to 20 036 M^{-1} Toxicity studies have been omitted for the derivative of CDs themselves. On the other hand, toxicity of CDs and their derivatives is very well documented in the literature [19,20].

In the present study, we compare the complexing abilities of recently synthesized derivatives of CDs [15] possessing the aromatic substituents connected via triazole group (Scheme 1). Voltammetric and spectroscopic studies reveal that the complexing abilities of these conjugates can be tuned and employed for pH-selective binding of anthracycline drugs. Toxicity of the synthesized complex as well as of the complex components were tested by the

MTT assay on two cell lines, the human lung carcinoma and the human cervical cancer cell lines.

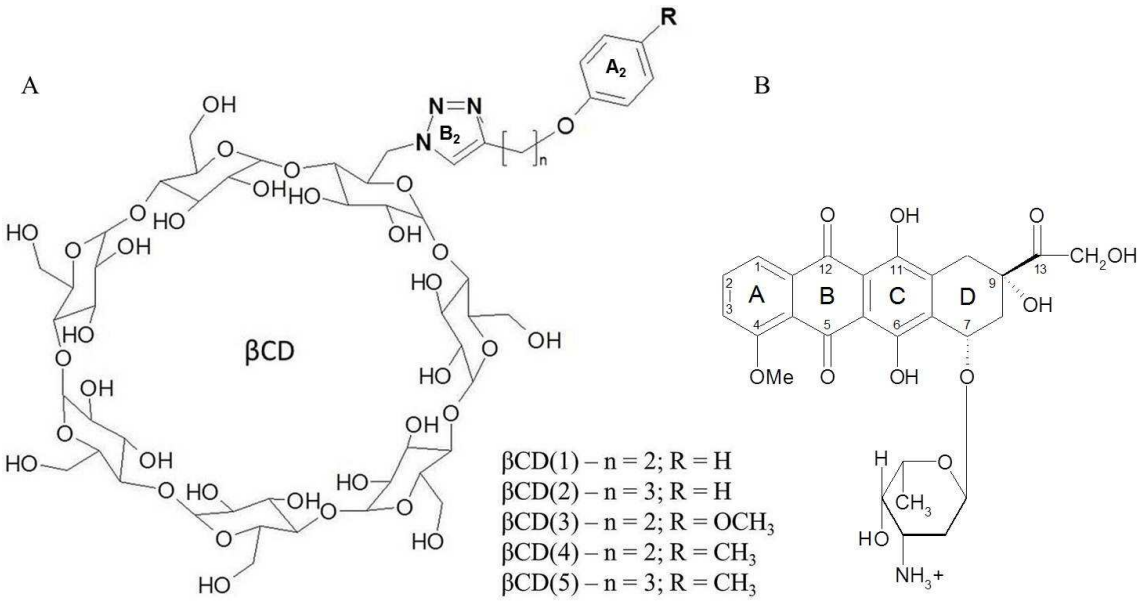

Scheme 1.

Materials and methods

Chemicals and Reagents. Doxorubicin hydrochloride salt was purchased from LC Laboratories (Woburn, USA). Other compounds used in this work for the syntheses were purchased from Aldrich and Fluka. The buffers were prepared using water from a Milli-Q ultrapure water system. Britton-Robinson buffer (BR, pH = 7.4 and pH = 5.5) was prepared in the usual way by the addition of appropriate amounts of 0.2 M sodium hydroxide to orthophosphoric acid, acetic acid and boric acid (0.04 M solutions). The pH was measured using pH-Meter E2 (Mettler Toledo). Because of the limited solubility of βCD complexes in water, all voltammetric and spectroscopic experiments were conducted in a mixture of Britton−Robinson buffer and DMSO (2:1 ratio). Concentration of Dox was the same in all the

experiments ($5 \cdot 10^{-5}$ M), while the concentration of CD derivatives was increased from $2.50 \cdot 10^{-4}$ to $1.75 \cdot 10^{-3}$ M.

Electrochemical Measurements. Electrochemical measurements were performed using a PGSTAT Autolab (Eco Chemie BV, Utrecht, Netherlands). All electrochemical experiments were performed in a three-electrode arrangement with a silver/silver chloride (Ag/AgCl) electrode (BASi) in a saturated solution of KCl as the reference, platinum foil as the counter and an Au electrode (BASi, 1.6 mm diameter) or GC electrode (BASi, 3 mm diameter) as the working electrodes. The working electrodes were polished mechanically with 1.0, 0.3, and 0.05 μm alumina powder on a Buehler polishing cloth. Prior to measurements, the buffer solutions were purged with purified argon for 15 min, and all experiments were performed at room temperature. Milli-Q ultrapure water (resistivity 18.2 MΩ/cm) was used.

Molecular Modeling. All theoretical calculations were performed with YASARA [21] using force field AMBER03 [22] with 7.86 A force cutoff and Particle Mash Ewald algorithm [23] to treat long range electrostatic interaction. The system was computed in the NPT ensemble with periodic boundary conditions, pressure 1 bar and temperature 298 K. The configuration consisted of 2711 atoms including CD, the hydrochloride salt of Dox, and water (TIP3P water model used). During the preparation stage atoms were parametrized and partial charges were assigned using semiempirical methods [24]. Each simulation lasted 100 ns and was preceded by energy minimization starting with steepest descent algorithm and followed by simulated annealing (time step 2 fs, atom velocities scaled down by 0.9 every 10th step) until convergence was reached. Several system configurations were considered including Dox placed inside CD and Dox at the entrance of CD. π–π interaction histograms were calculated from CD-Dox complex geometry.

Spectroscopic Measurements. UV−VIS spectroscopic measurements were performed using the EVOLUTION60 spectrophotometer with a 1 cm acryl cell.

Calculation of Formation Constants Voltammetric Data. Dox is electroactive and two pairs of peaks can be easily resolved in the cyclic voltammogram (Figure 1). Cyclic voltammetry was therefore, employed for the calculation of formation constants of the Dox−CDcomplexes based on the Osa equation [25]:

$$I_{obs}^2 = \frac{(I_{Dox}^2 - I_{obs}^2)}{K_s \cdot [CD]} + I_{DoxCD}^2 \qquad /1/$$

where I_{obs} is the reduction peak current /A/, Red_2 and I_{Dox} and $I_{Dox:CD}$ are the reduction peak currents for the free Dox and the inclusion complex, respectively. K_s is the complex formation constant, and [CD] is the concentration of the cyclodextrin. The value of K_s was calculated from the slope of the linear plot of I_{obs}^2 vs $(I_{Dox}^2 - I_{obs}^2)/[CD]$. All calculations were carried out for reduction peak current (Red_2) of the quinone group of doxorubicin, (Figure 1).

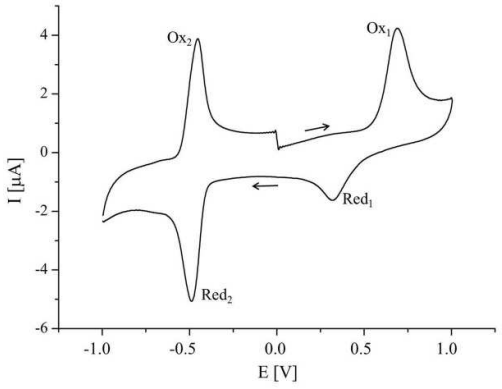

Figure 1.

Solubility of the compounds. The solubility of Dox was determined by LC Laboratory (Woburn, USA) at 10 mg/mL and 100 mg/mL in water and DMSO, respectively. The

solubility of native βCD in water is well known and is equal to18.5 mg/mL. The solubility increases in an irregular manner after the addition of DMSO. At less than 30% DMSO, the solubility remains constant (20 mg/mL). Between 30 and 40% of DMSO, the solubility rapidly increases to 770 mg/mL and remains constant up to 86% [26]. The solubility of βCD(1-5) were determined using UV−vis spectroscopy. The values for the solubility in pure water are less than that of native βCD and equal to 1.15 mg/mL, 0.91 mg/mL, 2.61 mg/mL, 1.12 mg/mL and 1.28 mg/mL for βCD(1), βCD(2). βCD(3), βCD(4) and βCD(5), respectively. Because of the limited solubility of βCD complexes in water, all experiments were conducted in a mixture of Britton−Robinson buffer and DMSO (2:1 ratio).

MTT assay. MTT (3-(4,5-dimethyldiazol-2-yl)-2,5 diphenyl tetrazolium bromide) test which measures activity of mitochondrial dehydrogenases was used to measure the short term cellular viability and was carried out as described in literature [27]. Human epithelial lung carcinoma cell line A549 and human cervix carcinoma cell line HeLa were purchased from the American Type Tissue Culture Collection (ATCC, Rockville, MD, USA) and cultured in F12 and DMEM medium, respectively, supplemented with 10 % fetal calf serum (Gibco), 100 units/mL penicillin and 100 μg/mL streptomycin. The cells were incubated in a 5 % CO_2 atmosphere at 37 °C. Cells were plated at 50 000 cells per well in 96-well plates in 200 μL of culture medium and were incubated at 37 °C for 24 h. After incubation, the medium was removed and 200 μL aliquots of fresh medium containing the tested compound in concentration 3.5 x 10^{-5} M or 1.25 x 10^{-5} M or vehicle (control) was added to plate wells. The stock solutions of the compounds studied were prepared by dissolving the appropriate amount of the compound in DMSO. Before experiment the stock solution was diluted 100 times in the appropriate medium and then mixed with cells with 1:1 ratio. Thus, the final concentration of DMSO in plate well containing cells was 0.5 %. Although no toxic effect of

0.5 % DMSO was observed in our experimental setup, the control samples also contained 0.5 % DMSO.

The plate was further incubated for 24 h or 48 h at 37 ^{o}C in a 5 % CO_2 humidified atmosphere. After incubation, 20 μL of MTT (5 mg/ml in PBS, pH 7) was added to each well. Cells were incubated at 37 °C for 4 h in a 5 % CO_2 humidified atmosphere. Then, the growth medium was removed, 100 μL of DMSO was added to each well to dissolve the purple crystals of formazan. The absorbance was measured in a plate reader spectrophotometer (Infinite M200, Tecan, USA) at a wavelength of 570 nm. The cell metabolic activity that roughly relates to the cell viability was expressed as ratio of absorbance of treated cells to the absorbance of the cells treated with vehicle, both after subtraction of the reagent control and multiplied by 100 %.

Results and Discussion

Upon addition of βCD derivatives to the solution of Dox, the decrease in anodic and cathodic peaks was observed (Figure 1), due to the smaller diffusion coefficient of the Dox–βCD complex, compared to that of the free guest. The formation constants of βCD derivatives – Dox complexes were calculated using Equation 1. Figure 2 shows the dependence of I^2_{obs} vs. $\frac{(I^2_{Dox} - I^2_{obs})}{[CD]}$ for βCD(2) at pH 7.4 and pH 5.5.

The value of formation constants for all of the complexes in pH 7.4 and pH 5.5 are depicted in Table 1.

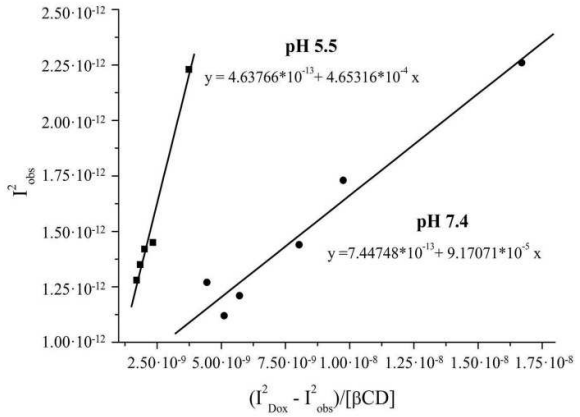

Figure 2.

At pH 7.4, corresponding to the pH of body fluids, the stability constants of complexes are large compared with those obtained for pH 5.5, characteristic for the cancer cells. Similar dependencies were obtained for all derivatives of βCD. The differences in stability constants at pH 7.4 and 5.5 are most significant for phenyl derivatives βCD(1) and βCD(2) and crezol derivative with a longer linker βCD(5). The still high stability constant at pH 5.5 does not allow, however, for the release of the drug in the tumor cells and, therefore, βCD(5) cannot be considered as a potential carrier for Dox. CD do not penetrate biological membranes.

As we have shown recently, the primary effect in the βCD-Dox complexes is strong proton-acceptor π–π interactions between the aromatic phenyl and triazole rings of the CD side group and ring A of doxorubicin.[15] At neutral pH (7.4), the electron-poor anthraquinone group strongly interacts with the electron rich triazole linker of βCD. At lower pH, the hydrogen cations interact with the free electron pairs on nitrogen atoms of the triazole group. This reduces electron density of the triazole ring and thereby weakens the proton-acceptor π–π interactions. On the other hand, the protonation of quinone and hydroquinone groups changes also the electron density distribution in Dox, which may also affect the CD-Dox interaction.

Table1. Formation constants of Dox–βCD derivatives complexes.

βCD derivative	Formation constants [M^{-1}]	
	pH 5.5	pH 7.4
βCD(1)	1837	10130
βCD(2)	2158	10871
βCD(3)	1079	2205
βCD(4)	3295	5990
βCD(5)	11955	32232

The stability constants of the Dox–βCD complexes depend both on the type of substituent on the aromatic ring in the side group of CD, and on the length of the hydrocarbon linker. The CDs with substituents providing electron density to the aromatic ring, e.g. methyl group in βCD(5), form stronger complexes with Dox than those without substituents in the ring, e.g. βCD(2) both at pH 5.5 and 7.4. The linker shorter by one $–CH_2–$ group causes a significant decrease in the value of stability constant of the Dox–βCD complex, as shown for βCD(3) and βCD(4). However, for βCD(1) with two methyl groups in the linker no significant changes in the stability constants were observed as compared with βCD(2) possessing a longer linker.

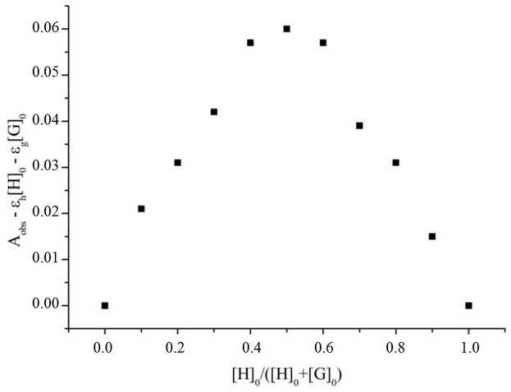

Figure 3.

The stoichiometric ratio of components in the complex was evaluated from the Job plots. We have examined a series of solutions of varying concentrations of βCD in a way that the total number of moles was kept constant. The dependence of the reduced absorption ($A_{obs} - \varepsilon_h[H]_0 - \varepsilon_g[G]_0$), where H is the host - βCD(2), and G is the guest – doxorubicin were evaluated from the maximum of Dox absorption ($\lambda_{Dox\text{-}max}$ = 255nm) or βCD(1-5) – $\lambda_{CD\text{-}max}$ different for each of the derivatives. Jobs plot measured for wavelength of 255 nm for βCD(2) is shown in Figure 3. The values of molar absorptivity for all compounds at relevant wavelengths are collected in Table 2. The stoichiometry of all of the complexes was found to be 1:1.

Table 2. The values of molar absorptivity for Dox and all βCD derivatives at $\lambda_{Dox\text{-}max,}$ and for Dox and all βCD at $\lambda_{max\text{-}CD}$ of each βCD derivatives.

Compound	ε at λ_{255}	ε at λ_{290}	ε at λ_{278}	ε at λ_{267}	ε at λ_{267}	ε at λ_{277}
CD(1)	902					1317
CD(2)	850			1731		
CD(3)	810	1789				
CD(4)	791				1876	
CD(5)	1090		1446			
Dox	14703					

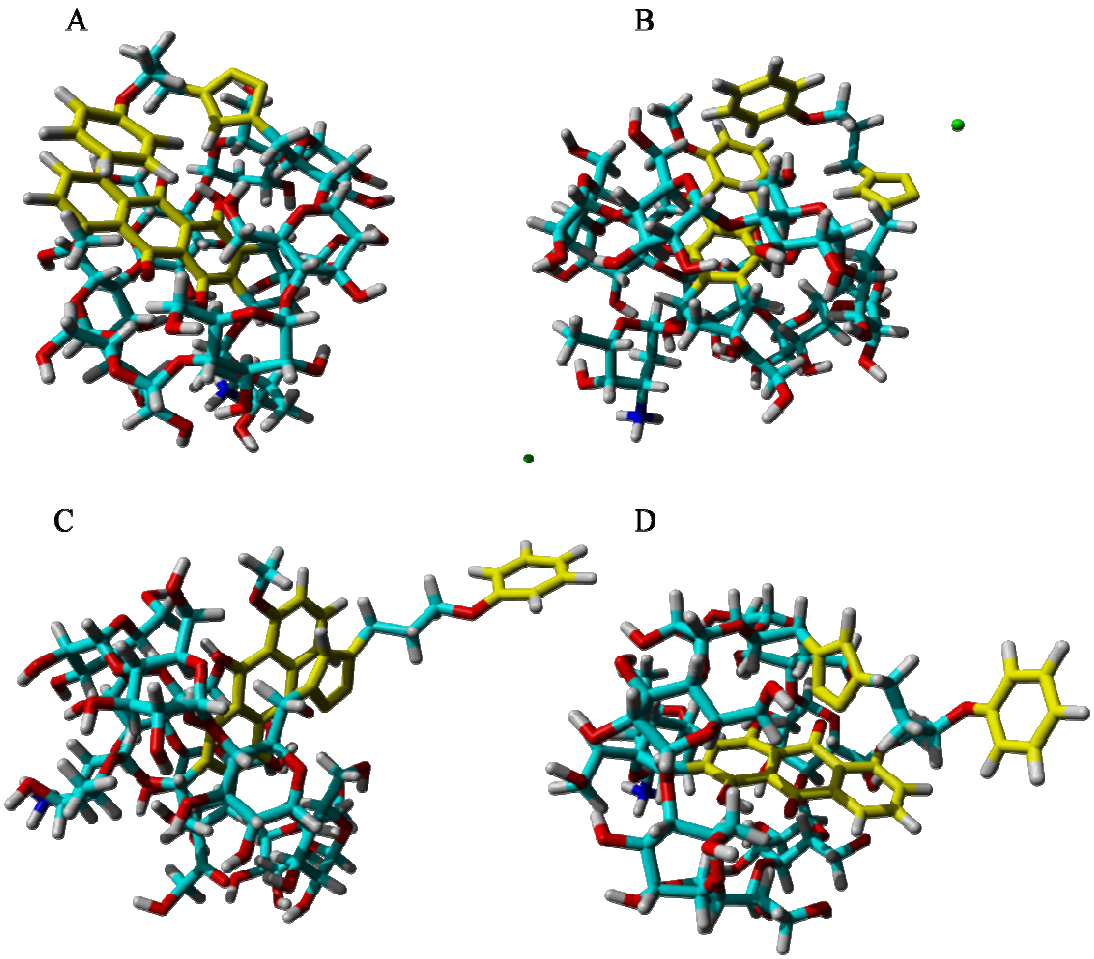

Figure 4.

Molecular modeling of the Dox–βCD(2) system revealed different interactions possible between Dox and βCD due to the presence of two aromatic rings in the side arm of βCD (Figure 4). The most expected π–π interaction between the ring A of Dox and the ring A_2 of side arm (see Scheme 1) of βCD can occur through "parallel-stacked" interaction (Figure 4A) and through the "T-shaped" interaction, when one ring is perpendicular to the other one (Figure 4B). In addition, molecular modeling shows interactions between the aromatic triazole linker B_2 and ring A or B of Dox (Scheme 1) by means of the "parallel-stacked" and "T-

shaped" impacts. Analysis of tilt angles of the aromatic rings A–A_2, A–B_2 and B–B_2 revealed that the favorable structure is the T-shaped interaction. In addition, the analysis of distances separating aromatic pairs R_{cen} indicates that dominant effects in the Dox–βCD (2) complex are interactions between ring B_2 of βCD and rings A or B of Dox (Figure 4C and 4D). As shown in the histograms of Figure 5, the average lengths for the A–B_2 and B–B_2 are significantly larger than that for A–A_2, but the dispersion is higher in the latter. This result may explain the lack of changes in the stability constant of the Dox–βCD complexes for βCD(1) and βCD(2) when the linker is shorter by one –CH_2– group. In addition, the values of the average distance for A–B_2 and B–B_2 aromatic pairs points to the T-shaped interaction since it appears at about 5.8 Å (Figure 5). This value is similar to the common distance for two benzene rings in biological systems such as protein witch aromatic amino acids (phenylalanine, tyrosine, histidine and tryptophan) which is approximately 5.1 Å [28, 29]. The higher value of the average distance may be due to some steric restrictions of the βCD side chain, when approaching the B_2 aromatic ring to the anthraquinone group of Dox.

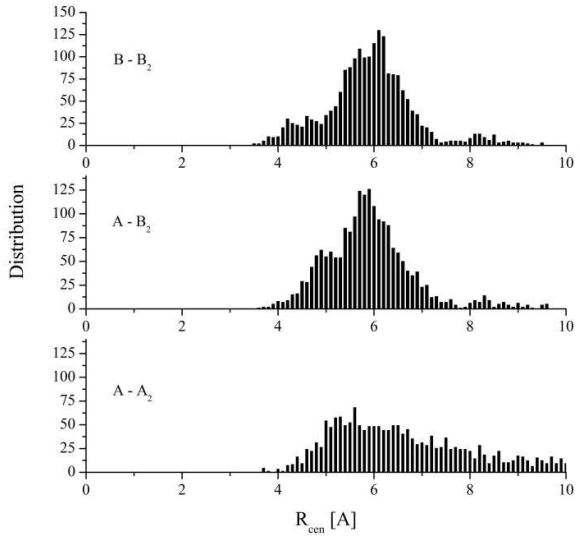

Figure 5.

To elucidate toxicity of the tested compounds and their complex we used two cells lines differing in response to xenobiotics. Due to the mutation the human lung carcinoma A549 cells have overstimulated the xenobiotic stress response through NRF/KEAP signaling pathway [30]. The A549 cells also show a strong response to the "survival type" signaling pathways that makes them more resistant to apoptotic stimuli [31]. As expected, the A549 cells proved to be less sensitive to all tested compounds than the HeLa cells. Nonetheless, both cell lines showed a clear time-dependent response to all tested compounds, with a the highest sensitivity to Dox–βCD(2) complex. A synergistic toxic effect of the Dox–βCD(2) complex was clearly visible in the HeLa cells after 24 h and in the A549 cells after 48 h treatment.

Cyclodextrins are usually used as drug carriers to improve: the drug solubility, absorption/bioavailability, stability, to control the drug release kinetics, provide site-specific drug delivery, or to reduce drug toxicity. Indeed, the complexes of CDs with Dox have lower toxicity then Dox alone. Interestingly, the toxicity of different Dox-CD complexes is proportional to the fraction of Dox released from the complex.[32] Since we observed synergistic toxic effect of the synthesized complexes, it seems plausible to assume that DOX is liberated from the complex and the observed toxicity results from the toxicity of DOX and βCD alone.

Whereas, the overall pattern of cellular response to the Dox–βCD (2) complex was similar in both cell lines tested, the cell lines responded in a different manner to the Dox and βCD(2) given alone. The A549 cells were more sensitive to βCD (2), whereas the HeLa cells were more sensitive to Dox (Figure 6).

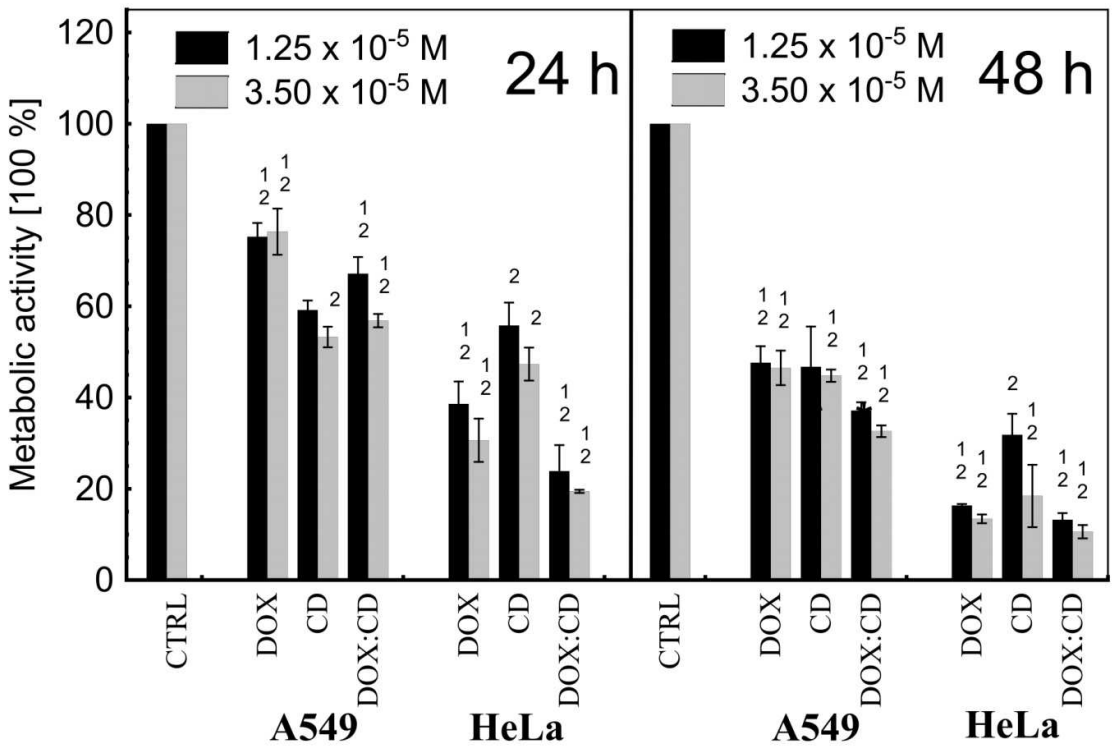

Figure 6.

The difference between cell lines is also easily visible, when the toxic effect of the tested compounds is compared. The toxicity of the tested compounds and their complex was between about 3.5 times to 1.5 time higher in the HeLa cells than the A549 cells in cells treated for 24 h, and between about 8 times to 0.5 times higher in cells treated for 48 h, depending on concentration and compound compared. This may reflect either the differences in cellular "preparedness" to the xenobiotic stress or the differences in cellular uptake of the tested compounds.

Conclusion

In this study, we demonstrate that newly synthesized derivatives of βCDs containing aromatic side arm connected by triazole group form strong inclusion complexes with Dox,

with stoichiometry 1:1. The structures and strengths of the complexes depend on the structure of the substituent the type and length of the linker. The βCD(5) with electron-rich aromatic ring forms a stronger complex with Dox than βCD(2) which does not have substituents in the aromatic ring of the side arm. For most derivatives, shorter linker results in a significant decrease of the stability constant, while for the phenyl derivatives βCD(1) and βCD(2) the shorter chains do not affect the stabilities.

The stability constants of the complexes depend on the pH of the solution. At pH 7.4, corresponding to the pH of body fluids, the stability constants are larger than those at pH 5.5, which is characteristic for cancer cells. At pH 5.5 the stability constants of the complexes formed are not much higher than the stability constants of the complex between Dox and native βCD. Molecular modeling done for the Dox–βCD(2) complex indicate that the dominant effects in the complex are the interactions between aromatic triazole linker of βCD(2) and anthraquinone rings of Dox. A synergistic toxic effect of the Dox–βCD complex clearly visible in both HeLa and A549 cancer cells likely indicates the release of doxorubicin from the cyclodextrin in the presence of pathologically changed cells.

Acknowledgements:

This work was supported by grant PSPB 079/2010 from Switzerland through the Swiss Contribution to the enlarged European Union. O.S. thanks National Science Center for support through Project 2011/01/N/ST5/05550.

Figure Captions

Figure 1. Voltammetric curve of Dox ($5 \cdot 10^{-5}$ M) recorded in BR buffer at pH 5.5. Scan rate 0.2V/s.

Figure 2. The plots of the Osa eq. 1 for Dox in the presence of βCD(2) recorded in Britton−Robinson buffer : DMSO (2:1) at pH 7.4 (A) and 5.5 (B).

Figure 3. Job plots for Dox–βCD(2) complex calculated from UV-VIS experiments. Stock solutions $1 \bullet 10^{-4}$ M.

Figure 4. Molecular modeling of the βCD(2) interactions with Dox in water. Aromatic components are colored in yellow. Structures description in the text.

Figure 5. Histograms of R_{cen} counts for aromatic pairs: $A–A_1$, $A–B_2$ and $B–B_2$ for a 2000 frames of simulation.

Figure 6. Toxicity of the synthesized complex Dox-βCD(2) and its components as measured by MTT assay. All results of treated cells were significantly lower than control. 1 – denotes statistically significant difference of means between A549 and HeLa cells for given compound, time and concentration; 2 – denotes statistically significant difference of means between 24 h and 48 h for given compound, cell line and concentration. Student's t test, $p < 0.05$, $n = 3$.

Scheme

Scheme 1. The structures of: (A) βCD(1-5) and (B) Dox.

Table

Table 1. Formation constants of Dox–βCD derivatives complexes.

Table 2. The values of epsilon for Dox and βCD derivatives at $\lambda_{Dox\text{-}max,}$, and for Dox and all βCD derivatives at $\lambda_{max\text{-}CD}$ of each of the βCD derivatives.

***Corresponding Author**[*] bilewicz@chem.uw.edu.pl

[1] Chaires, J. B.; Herrera, J. E.; Waring, M. J. Preferential Binding of Daunomycin to 5'ATCG and 5'ATGC Sequences Revealed by Footprinting Titration Experiments. *Biochemistry* **1990**, 29, 6145–6153.
[2] Steinherz, L. J.; Steinherz, P. G.; Tan, C. T.; Heller, G.; Murphy, M. L. Cardiac Toxicity 4 to 20 years after Completing Anthracycline Therapy. *J.A.M.A.* **1991**, 266, 1672–1677.
[3] Tinkov, S.; Winter, G.; Coester, C.; Bekeredjian, R. New Doxorubicin-loaded Phospholipid Microbubbles for Targeted Tumor Therapy: Part I - Formulation Development and in-vitro Characterization. *J. Controlled Release* **2010**, 143, 143–150.
[4] Šimùnek, T.; Štìrba, M.; Popelová, O.; Adamcová, M.; Hrdina, R.; Geršl, V. Anthracycline-induced Cardiotoxicity: Overview of Studies Examining the Roles of Oxidative Stress and Free Cellular Iron. *Pharmacological Reports.* **2009**, 61, 154–171.
[5] Nawara, K.; McCracken, J. L.; Krysinski, P.; Blanchard, G.J. Structure-Dependent Complexation of Fe3+ by Anthracyclines. 1. The Importance of Pendant Hydroxyl Functionality, *J. Phys. Chem. B* **2013**, DOI: 10.1021/jp402349e
[6] Nawara, K.; McCracken, J. L.; Krysinski, P.; Blanchard, G.J. Structure-Dependent Complexation of Fe3+ by Anthracyclines. 2. The Roles of Methoxy and Daunosamine Functionalities. *J. Phys. Chem. B* **2013** DOI: 10.1021/jp4023508
[7] Nawara, K.; Krysinski, P.; Blanchard, G.J. Photoinduced Reactivity of Doxorubicin: Catalysis and Degradation, *J. Phys. Chem. A* **2012**, 116, 4330−4337.
[8] Nawara, K.; Krysinski, P.; Blanchard, G.J. Doxorubicin is a Photocatalyst for the Generation of H_2O_2, *RSC Advances* **2012**, 2, 4059–4061.
[9] Husain, N.; Ndou, T. T.; Munoz De La Pena, A.; Warner, I. M. Complexation of Doxorubicin with β- and γ-Cyclodextrins, *Applied Spectroscopy* **1992**, 46, 652-658.
[10] Brewster, M. E.; Loftsson, T.; Estes, K. S.; Lin, J. L.; Fridriksdottir, H.; Bodor, N. Effects of Various Cyclodextrins on Solution Stability and Dissolution Rate of Doxorubicin Hydrochloride, *Int. J. Pharm*. **1992**, 79, 289-299.
[11] Schneider, Y.J.; Baurain, R.; Zenebergh, A.; Trouet, A. DNA-binding Parameters of Daunorubicin and Doxorubicin in the Conditions used for Studying the Interaction of Anthracycline-DNA Complexes with Cells in vitro, *Cancer Chemother Pharmacol* **1979**, 2, 7-10.
[12] Yamanoi, T.; Yoshida, N.; Oda, Y.; Akaike, E.; Tsutsumida, M.; Kobayashi, N.; Osumi, K.; Yamamoto, K.; Fujita, K.; Takahashi, K.; Hattori, K. Synthesis of Mono-glucose-branched Cyclodextrins with a High Inclusion Ability for Doxorubicin and their Efficient Glycosylation using Mucor Hiemalis endo-β-N-Acetylglucosaminidase. *Bioorganic & Medicinal Chemistry Letters* **2005**, 15, 1009–1013.
[13] Oda, Y.; Kobayashi, N.; Yamanoi, T.; Katsuraya, K.; Takahashi, K.; Hattori, K. Beta-cyclodextrin Conjugates with Glucose Moieties Designed as Drug Carriers: Their Syntheses, Evaluations using Concanavalin A and Doxorubicin, and Structural Analyses by NMR spectroscopy. *Med.Chem*. **2008**, 4, 244-255.
[14] Kralova, J.; Kejik, Z.; Briza, T.; Pouckova, P.; Kral, A.; Martasek, P. Kral, V. Porphyrin-cyclodextrin Conjugates as a Nanosystem for Versatile Drug Delivery and Multimodal Cancer Therapy, *J.Med.Chem.* **2010**, 53, 128-138.
[15] Swiech, O.; Mieczkowska, A.; Chmurski, K.; Bilewicz, R. Intermolecular Interactions between Doxorubicin and β-Cyclodextrin 4-Methoxyphenol Conjugates. *J. Phys. Chem. B* **2012**, 116, 1765−1771.
[16] Martin, F. *Clinical Pharmacology and Antitumor Efficacy of DOXIL (Pegylated Liposomal Doxorubicin)* in Lasic, D. D. Papahadjopoulos D. (Eds) *Medical Applications of Liposomes*, Elsevier, New York 1998 pp. 635-688.
[17] Hrubý, M.; Koňak, Č.; Ulbrich, K. Polymeric Micellar pH-sensitive Drug Delivery System for Doxorubicin. *J. Controlled Release* **2005**, 103, 137–148.
[18] Li, L.; Zhao, M.; Li, W.; Wang, Y.; Zhang, Z.; An, R.; Peng, S. Self-complexation and Complexation-controlled Target Cancer Therapy. *Med. Chem. Commun*. **2012**, 3, 1059–1061.
[19] Irie, T.; Uekama, K. Pharmaceutical Applications of Cyclodextrins. III. Toxicological Issues and Safety Evaluation. *J. Pharm. Sci*. **1997**, 86, 147-162.
[20] Uekama, K.; Hirayama, F.; Irie, T. Cyclodextrin Drug Carrier Systems, *Chem. Rev.* **1998**, 98, 2045-2076.
[21] Krieger, E.; Darden, T.; Nabuurs, S.; Finkelstein, A.; Vriend, G. Making optimal use of Empirical Energy Functions: Force-field Parameterization in Crystal Space, *Proteins* **2004**, 57, 678−683.
[22] Duan, Y.; Wu, C.; Chowdhury, S.; Lee, M.C.; Xiong, G.; Zhang, W.; Yang, R.; Cieplak, P.; Luo, et. all. A Point-charge Force Field for Molecular Mechanics Simulations of Proteins based on Condensed-phase Quantum Mechanical Calculations. *J. Comput. Chem.* **2003**, 24, 1999−2012.
[23] Essman, U.; Perera, L.; Berkowitz, M.L.; Darden, T.; Lee, H.; Pedersen, L.G. A Smooth Particle Mesh Ewald Method, *J.Chem.Phys.B* **1995**, 103, 8577-8593.

[24] Jakalian, A.; Jack, D.B.; Bayly, C.I. Fast, Efficient Generation of High-quality Atomic Charges. AM1-BCC Model: II. Parameterization and Validation, *J. Comput. Chem.* **2002**, 23 ,1623−1641.
[25] Osa, T.; Matsue, T.; Fujihira, T. Cyclodextrin-Nitrophenol Systems Studied by Polarography, Heterocycles **1977**, 6, 1833−1839.
[26] Chatijgakis, A.K.; Donze, C.; Coleman, A. W. Solubility Behavior of β-cyclodextrin in Water/Cosolvent Mixtures, *Anal. Chem.* **1992**, 64, 1632−1634.
[27] Fotakis, G.; Timbrell, J.A. In vitro Cytotoxicity Assays-comparison of LDH, Neural Red, MTT and Protein Assay in Hepatoma Cell Lines Following Exposure to Cadmium Chloride, *Toxicol Lett.* **2006**, 160, 171-177.
[28] McGaughey, G.B.; Gagne, M.; Rappe, A.K. π–Stacking Interactions: Alive and Well in Proteins, *J. Biol. Chem.* **1998**, 273, 15458–15463.
[29] C.A. Hunter, J.K.M. Sanders, The Nature of π-π Interactions, J. Am. Chem. Soc. 112 (1990) 5525-5534.
[30] Singh, A.; Misra, V.; Thimmulappa, R.K.; Lee, H.; Ames, S.; Hoque, M.O.; Herman, J.G.; Baylin, S.B.; Sidransky, D.; Gabrielson, E.; Brock, M.V.; Biswal, S. Dysfunctional KEAP1-NRF2 Interaction in Non-Small-Cell Lung Cancer. *PLOS Med.* **2006**, 3, 1865-1876.
[31] Kastamoulas, M.; Chondrogiannis, G.; Kanavaros, P.; Vartholomatos, G.; Bai, M.; Briasoulis, E.; Arvanitis, D.; Galani, V. Cytokine Effects on Cell Survival and Death of A549 Lung Carcinoma Cells. *Cytokine* **2013**, 61, 816-825.
[32] Tanaka, H.; Kominato, K.; Yamamoto, R.; Yoshioka, T.; Nishida, H.; Tone, H.; Okamoto, R. Synthesis of Doxorubicin-Cyclodextrin Conjugates , *J. Antibiot.* **1994**, 47, 1025-1029,

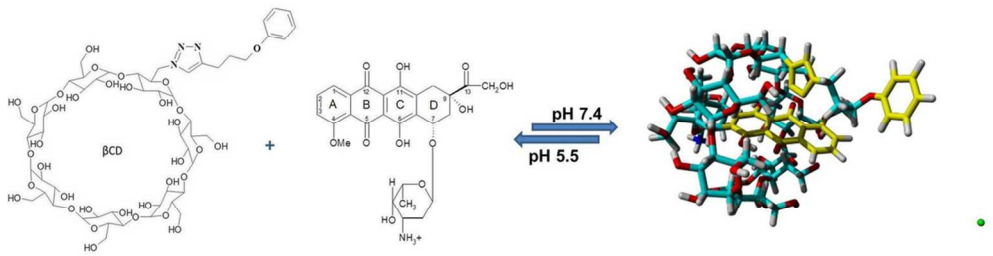

graphical abstract
49x17mm (600 x 600 DPI)